Supporting Information

High-Throughput Fabrication of High Aspect Ratio Ag/Al Nanopillars for Optical Detection of Biomarkers

Ainash Garifullina* and Amy Q. Shen*

Micro/Bio/Nanofluidics Unit, Okinawa Institute of Science and Technology Graduate University, 1919-1 Tancha, Onna-son, Okinawa, 904-0495 Japan

E-mail: ainash.garifullina@oist.jp; amy.shen@oist.jp

Contents

S1. Reusability of the PDMS – filled AAO templates for fabrication of PS nanopillars and their aspect ratios

After using the PDMS–filled AAO templates for fabrication of PS nanopillars, we tested the reusability of these templates. Fig. S1 shows the average aspect ratios of PS nanopillars after each trial of reusing the same AAO template (5 total reuses), whereas Fig. S2 shows SEM images of the PS nanopillars formed by reusing the same PDMS – filled template. Based on our calculations, the PDMS – filled AAO templates can be reused at a minimum of five times since the average aspect ratio of the PS nanopillars remains approxinately the same.

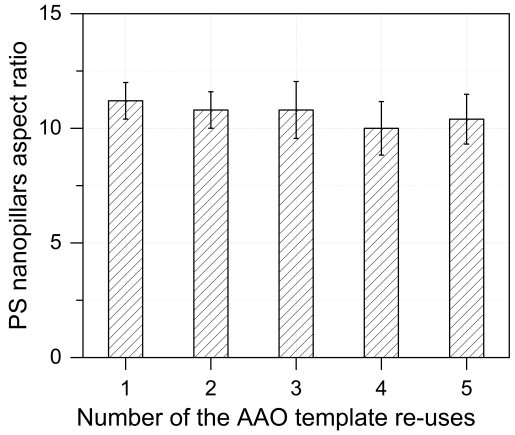

Figure S1: Average aspect ratio of PS nanopillars after reusing the same PDMS – filled AAO template each time, 5 times total (error bars represent standard deviation based on these five measurements).

Aspect ratios of the PS nanopillars were measured using cross section images. However, due to strong charging effects and difficulties with cutting the PS films without physically damaging the nanopillars, the number of possible ways to acquire high resolution cross-section images were limited. To be able to look at the cross section of the PS nanopillars, we initially immersed the PS films into liquid nitrogen. After which, we applied small amount of pressure from the top of the PS film causing it to break into a number of smaller pieces.

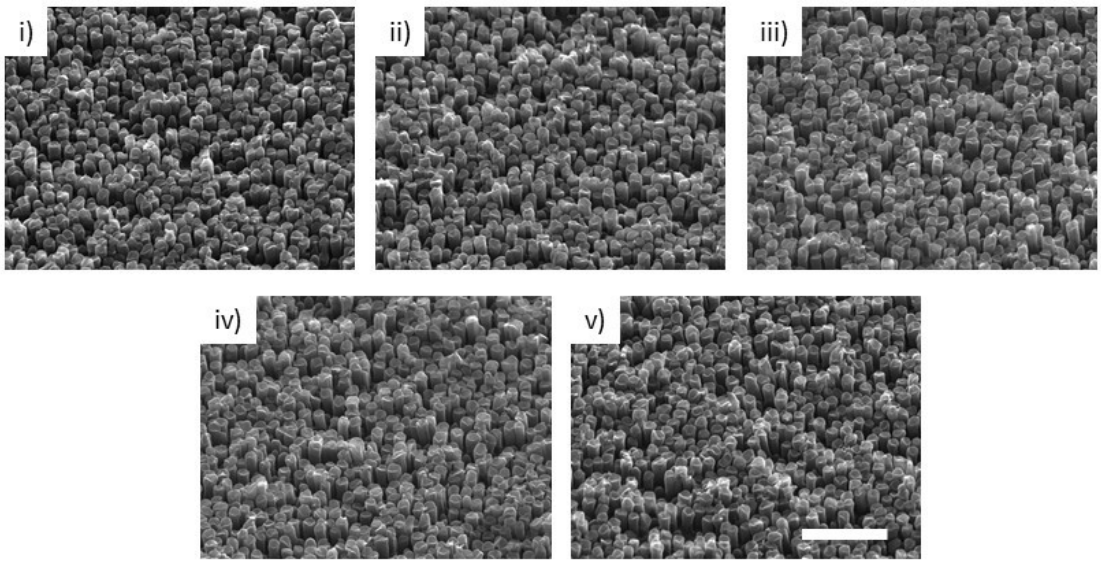

Figure S2: SEM images of PS nanopillars fabricated using the same PDMS – filled AAO template each time, scale bar $= 2\,\mu$m.

These smaller pieces, in turn, were viewed under SEM (FEI Quanta 250 FEG) to acquire cross-section images (Fig. S3(a) & (b)). The downside of this method is that some broken bits from the PS films also cracked many PS nanopillar tips, thereby the imaged structures (somewhat damaged with reduced height of the actual nanopillar) are not exactly the same as our original nanopillar structure.

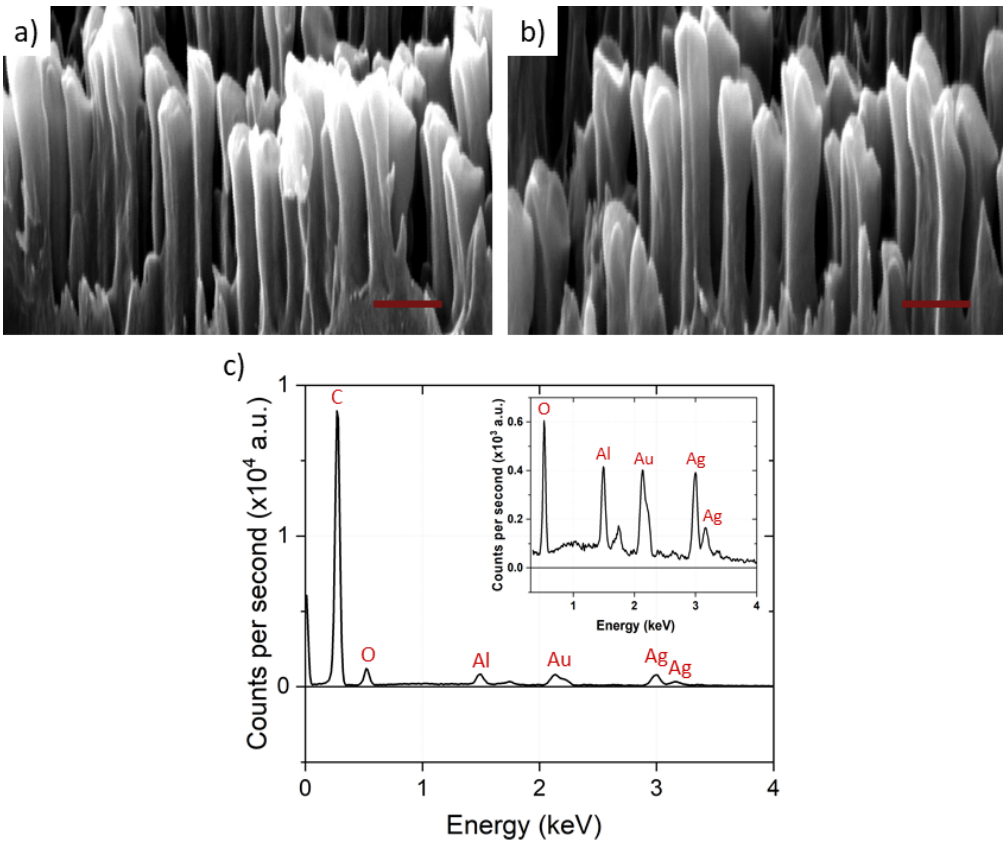

Figure S3: (a & b) SEM images of PS nanopillars fabricated by using PDMS–coated AAO templates subjected to 4 minutes TBA at 80°C, and acquired by freezing PS films in liquid nitrogen and then breaking them into smaller pieces, scale bar = 500 nm; c) EDS spectra of the cross-section of the Ag/Al-coated PS nanopillars.

S2. Collapsing of higher aspect ratio PS nanopillars

Although longer contact time (over 4 minutes) with hot TBA solvent resulted in higher aspect ratio PS nanopillars, as it can be seen from Fig. S4, nanopillars start to collapse and the surface of the PS nanofilm becomes notably less uniform. This can be explained by the fact that after 4 minutes the TBA solvent starts boiling, causing non-uniform temperature distribution and thus non-uniform removal of the excess PDMS mixture from the surface of the PDMS–coated AAO templates. This, in turn, leads to non-uniform PDMS–filled AAO templates and, consequently, to the PS nanopillars with non-uniform lengths.

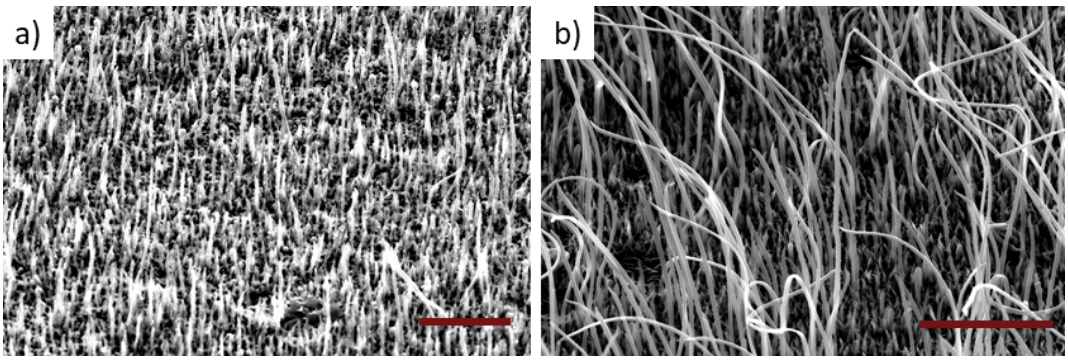

Figure S4: SEM images of collapsed PS nanopillars fabricated by using PDMS – coated AAO templates subjected to (a) 5 minutes TBA at 80°C; (b)10 minutes TBA at 80°C. The scale bar = 5 μm.

S3. LoD and LoQ calculations in PBS

To test biosensing performance of the developed Ag/Al–coated polystyrene (PS) nanopillars platform, we have detected six different concentrations of hCRP and SARS-CoV-2 spike protein diluted in both PBS and diluted human plasma. To calculate the limits of detection and quantification (LoD & LoQ), we used a standard approach[1] and plotted $\Delta\lambda_{\mathrm{LSPR}}$ against the concentration of the detected antigen measured in ng/mL. Fig. S5 represents wavelength shifts caused by detection of 0 – 1000 ng/mL hCPR in (a) and SARS-CoV-2 spike protein diluted in 0.01 M PBS in (c).

Since $\Delta\lambda_{\mathrm{LSPR}}$ had logarithmic dependence on concentration of both hCRP and SARS-CoV-2 spike protein, we considered only a low concentration range (from 0 to 10 ng/mL, insets on Fig. S6(a & b)) to estimate LoD and LoQ of the functionalized sensor surface. The best linear fit for hCRP detection in 0.01 M PBS (Figure S6a, inset) follows

$$\Delta\lambda_{\mathrm{LSPR}} = 1.3474 \times [\mathrm{C}] + 0.6359. \tag{S1}$$

The best linear fit for SARS-CoV-2 spike protein (Figure S6b, inset) detection in 0.01 M PBS follows

$$\Delta\lambda_{\mathrm{LSPR}} = 1.4687 \times [\mathrm{C}] + 2.3305. \tag{S2}$$

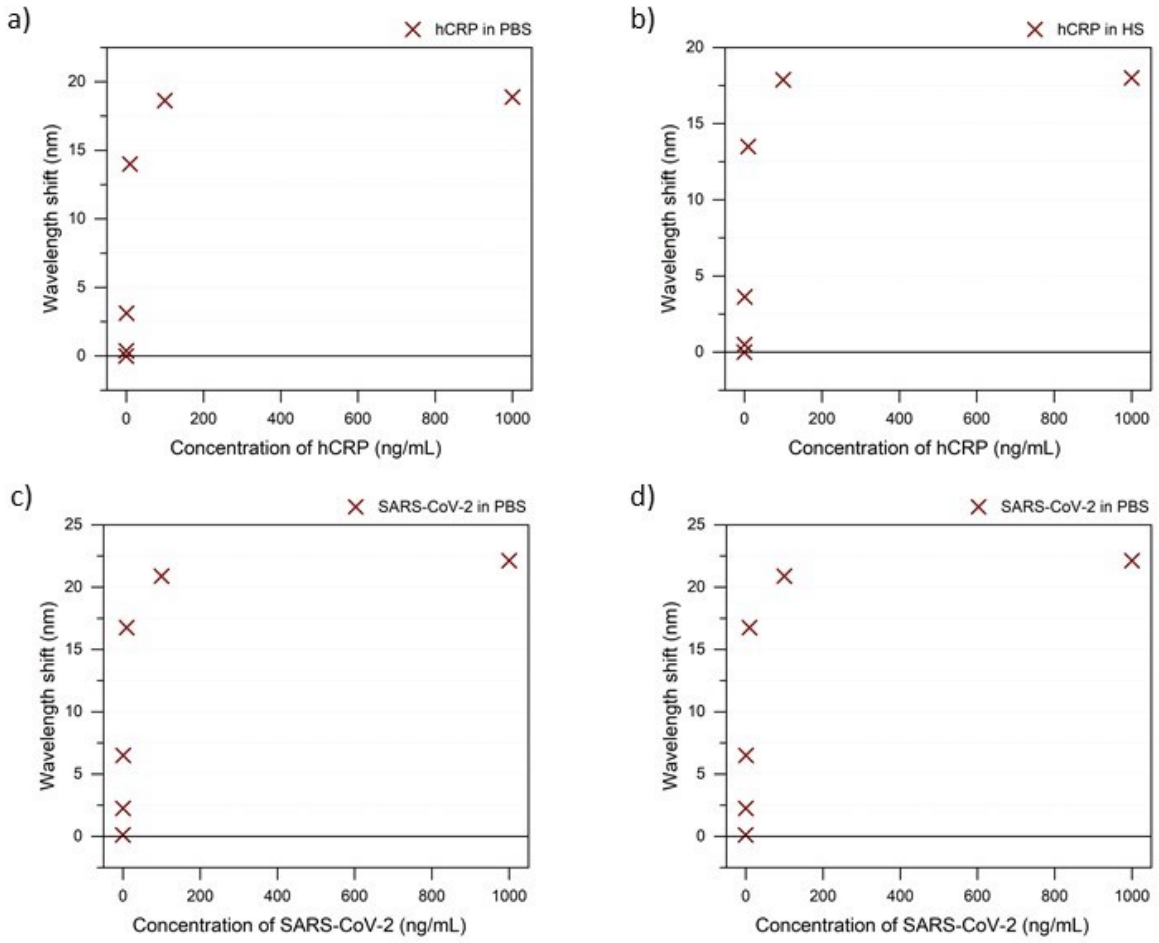

Figure S5: Wavelngth shifts (nm) plotted against six different concentrations of a) hCRP & c) SARS-CoV-2 spike protein (0, 0.1, 1, 10, 100, and 1000 ng/mL) diluted in human plasma (1 : 100 diluted in 0.01 M PBS). Insets represent linear plots in the 0 – 1000 ng/mL concentration range.

Slopes of these two equations, 1.35 and 1.47 ng/mL, indicate sensitivities of the developed Ag/Al–coated PS nanopillars platforms towards hCRP and SARS-CoV-2 spike protein diluted in PBS, respectively. Standard deviation of the blank (SD_{blank}, 0 ng/mL solution) was calculated using STEYX function in Excel and was found to be $SD_{blank} = 0.50$ ng/mL for hCRP and $SD_{blank} = 0.33$ ng/mL for SARS-CoV-2 spike protein. Using this, we calculated the LoD and LoQ as follows:[1,2]

$$\text{LoD} = 3.3 \times \frac{SD_{blank}}{\text{Slope}}, \tag{S3}$$

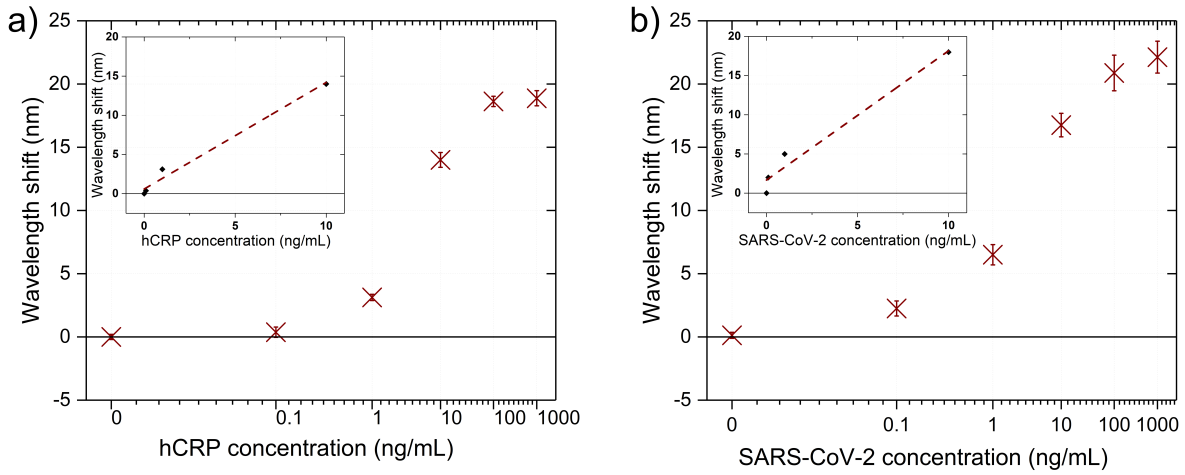

Figure S6: Wavelngth shifts (nm) plotted against six different concentrations of (a) hCRP; (b) SARS-CoV-2 spike protein (0, 0.1, 1, 10, 100, and 1000 ng/mL) diluted in 0.01 M PBS. Inserts represent linear plots in the 0 – 10 ng/mL concentration range.

$$\mathrm{LoQ} = 10 \times \frac{\mathrm{SD}_{blank}}{\mathrm{Slope}}. \tag{S4}$$

and found that LoD and LoQ for detection of hCRP in 0.01 M PBS are equal to 1.22 and 3.71 ng/mL (10 pM and 30 pM), respectively. Whereas, LoD and LoQ for SARS-CoV-2 spike protein in 0.01 M PBS are 0.74 and 2.25 ng/mL (4 pM and 12 pM).

S4. LoD and LoQ calculations in human plasma

Similarly, we used Ag/Al–coated PS nanopillars to detect six different concentrations of hCRP and SARS-CoV-2 spike protein diluted in human plasma (1 : 100 in 0.01 M PBS). The recorded wavelength shifts (nm) were plotted against the concentrations of the respective antigens as shown in Fig. S5. Based on the lower concentration range (from 0 to 10 ng/mL, insets on Fig. S7(b & d)), we plotted a standard addition line and got the following equations:

$$\Delta\lambda_{\mathrm{LSPR}} = 1.2786 \times [\mathrm{C}] + 0.8582 \tag{S5}$$

for hCRP (Figure S7a, inset) and

$$\Delta\lambda_{\mathrm{LSPR}} = 1.1698 \times [\mathrm{C}] + 2.5351 \tag{S6}$$

for SARS-CoV-2 spike protein (Figure S7b, inset) detection in human plasma. From these equations, the sensitivity of the developed platform was calculated to be 1.28 and 1.17 ng/mL towards hCRP and SARS-CoV-2 spike protein in diluted human plasma, respectively.

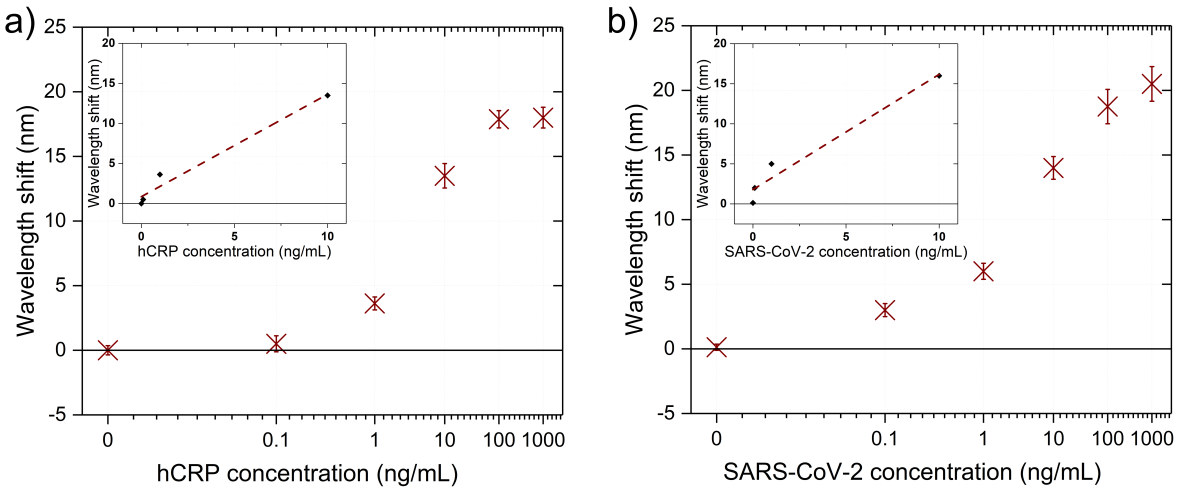

Figure S7: Wavelngth shifts (nm) plotted against six different concentrations of a) hCRP & b) SARS-CoV-2 spike protein (0, 0.1, 1, 10, 100, and 1000 ng/mL) diluted in human plasma (1 : 100 diluted in 0.01 M PBS). Insets represent linear plots in the 0 – 10 ng/mL concentration range.

Using equations S3 and S4, we calculated LoD and LoQ for detection of hCRP in human plasma to be 1.29 and 3.91 ng/mL (11 pM and 36 pM), respectively. LoD and LoQ for SARS-CoV-2 spike protein in human plasma was equal to 0.93 and 2.83 ng/mL (5 pM and 15 pM), respectively.

S5. Stability of the optical signal after antibody immobilization

To test if the LSPR signal detected from the surface of the Ag/Al-coated PS nanopillars remains stable throughout time, we immobilized 100 ng/mL hCRP antibody on the Ag/Al PS nanopillars and measured the UV-Vis spectra on days 1 through 5. We found that the wavelength shift $\Delta\lambda_{LSPR}$ value fluctuated within ± 1 nm (Figure S8), which is a very small value and therefore can be ignored.

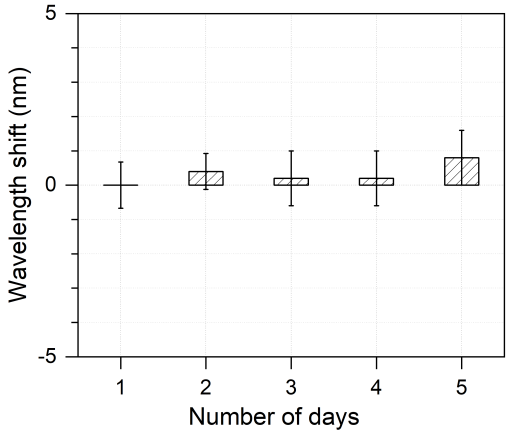

Figure S8: Wavelength shifts (nm) measured from the surface of five Ag/Al-coated PS nanopillars after immobilization of 100 ng/mL anti-hCRP on days 1, 2, 3, 4, and 5.

References

(1) Shabir, G. A. Validation of high-performance liquid chromatography methods for pharmaceutical analysis: Understanding the differences and similarities between validation requirements of the US Food and Drug Administration, the US Pharmacopeia and the International Conference on Harmonization. *Journal of Chromatography A* **2003**, *987*, 57–66.

(2) Shrivastava, A.; Gupta, V. B. Methods for the determination of limit of detection and limit of quantitation of the analytical methods. *Chron. Young Sci.* **2011**, *2*, 21.